International Journal of Pure and Applied Mathematics
Volume 120 No. 5 2018, 967-981
ISSN: 1314-3395 (on-line version)
url: http://www.acadpubl.eu/hub/
Special Issue

http://www.acadpubl.eu/hub/

Joule Heating and Thermal Radiation Effects on MHD Peristaltic Couple Stress Hemodynamic Fluid Model through an Inclined Channel with Chemical Reaction

S. Ravikumar[1§], J. Suresh Goud[2], P. Srilatha[3], R. Sivaiah[4], SK. Abzal[5]

[1, 4, 5]Department of Mathematics
NBKR Institute of Science and Technology (Autonomous)
Vidyanagar, SPSR Nellore, Andhra Pradesh, 524413, INDIA

[2,3]Department of Mathematics
Institute of Aeronautical Engineering (Autonomous)
Dundigal, Telangana, 500043, INDIA

Abstract

The aim of the present article deals with the joule heating and thermal radiation effects on MHD peristaltic couple stress hemodynamic fluid model through an inclined channel with chemical reaction. The porous medium is also taken into the account. The ensuing advanced mathematical system has been discussed for small Reynolds number and large wavelength concepts. Numerical results were presented for axial velocity, pressure gradient, pressure rise, frictional force, temperature and concentration. Variations of the said quantities with dissimilar parameters are computed by using MATHEMATICA software. Graphs reflecting the contributions of embedded parameters were discussed. It is worth mentioning that the pumping rate reduces in the entire retrograde region and also in peristaltic pumping zone while the pumping rate gradually increases in free pumping and co-pumping zones by increase in porosity parameter. It is observed that the frictional forces exactly have an opposite behavior when compared to the pressure rise. We notice that the temperature of the fluid enhances by an increase in hartmann number, prandtl number, brinkman number, heat source/sink parameter and couple stress parameter while it reduces by an increase in porosity parameter and thermal radiation parameter. It can be seen that the concentration of the fluid increases by the increase in thermal radiation parameter, porosity parameter and chemical reaction parameter while it decreases by an increase in schmidt number, soret number, prandtl number, hartmann number and couple stress parameter.

AMS Subject Classification: 92C10, 76S05, 92B05, 92C50,76Z05

Keywords: Thermal radiation; Chemical reaction; Hartmann number; Porous medium; Inclined channel; Joule heating; Mass transfer

1. Introduction

The study of peristaltic mechanism has become widespread among the researchers during the last few decades. Peristalsis has its monumental applications in medical physiology. In medical physiology, it's concerned with the motion of food material within the disagreeable person, as an example, within the propulsion of food bolus within the passage, conversion of food bolus into nutrient within the abdomen and movement of nutrient within the bowel, urine transport from kidney to bladder, semen movement in vas deferens, movement of lymphatic fluids in lymph vessels, bile flow from the gall bladder into the duodenum, vasomotion of blood cells, movement of ovum in the female fallopian tube and transport of spermatozoa in the ductus efferents.The study of couple stress fluid is very useful in understanding various physical problems because it possesses the mechanism to describe rheological complex fluids such as liquid crystals and human blood. By couple stress fluid, we mean a fluid whose particles sizes are taken into account, a special case of non-Newtonian fluids. Kill's [1] research work has given relevance to the physiological applications of peristalsis. Latham [2] and Shapiro et al. [3] discussed the peristalsis of viscous fluids through theoretical and experimental approaches. Studies on peristaltic flow under long wavelength approximation and small Reynolds number models were carried out by several investigators (Srinavasacharya et al. [4], Vajravelu et al. [5],Maiti and Misra [6], Ravikumar [7],Ravikumar [8], Ravikumar [9],Ravikumar and Abzal [10],Ameer Ahamad et al. [11],Sankad and Nagathan [12], Shit and Roy [13]).

In general heat transfer and mass transfer, play a vital role in MHD flows. When a fluid is at a different temperature from that of its surroundings, the thermal energy transfers from high temperature region to low temperature region until the fluid and the surroundings attain thermal equilibrium. This is called heat transfer or heat exchange. Apart from this, there are many industrial, chemical engineering processes, Automotive Engineering, Thermal Insulations, Thermal Engineering of electronic devices and system, Material Processing, Power Plant Engineering, Bio-hear Transfer, Aerospace Technology, etc. Kabir et al. [14] presented a theoretical study on effects of stress work on MHD natural convection flow along a vertical wavy surface with Joule heating. Hayat et al. [15] have conferred the characteristics of convective heat transfer in the MHD peristalsis of Carreau fluid with Joule heating. Abbasi et al. [16] discussedan effect of inclined magnetic field and Joule heating in the mixed convective peristaltic transport of non-Newtonian fluids.Influence of Thermal Radiation and force field on Peristaltic Transport of a Newtonian Nanofluid in a very Tapered uneven Porous Channel investigated by Kothandapani and Prakash [17].Ramesh [18] investigated an influence of heat and mass transfer on peristaltic flow of a couple stress fluid through porous medium in the presence of inclined magnetic field in an inclined asymmetric channel. In another paper, Hayat et al. [19] examined the radiative peristaltic flow of magneto nanofluid in a porous channel with thermal radiation.Maruthi Prasad et al. [20] investigated on heat and mass transfer effects of peristaltic transport of a nanofluid in peripheral layer. Effect of nonlinear thermal radiation on MHD chemicallyreacting maxwell fluid flow past a linearly stretching sheet studied by Mohan RamiReddy et al. [21].Siva and Govindarajan [22] analysed thesoret effect on peristaltic flow of a couple stress fluid in a tapered channel. MHD peristaltic flow of a couple stress fluid in an asymmetric channel discussed by Latha and Rushi Kumar [23].

2. Formulation of the problem

Let us consider the flow of an incompressible, viscous and electrically conducting peristaltic couple-stress fluid flowing through an inclined channel of uniform thickness under the action of an external magnetic field. Joule heating, thermal radiation, porous medium and chemical reaction are also taken into the account. The uniform channel width is taken as 2d and the

wave is considered to be moving at wave speed c. The temperature maintained at lower andupper walls are T_0 and T_1, respectively. The concentration fields associated withlower and upper walls are taken as $C_0$and C_1 respectively.

The wall deformation is given by

$$h(x, t) = d + a \sin \frac{2\pi}{\lambda}(x-ct), \quad (1)$$

where λ is the wave length, a is an amplitude of the channel walls.

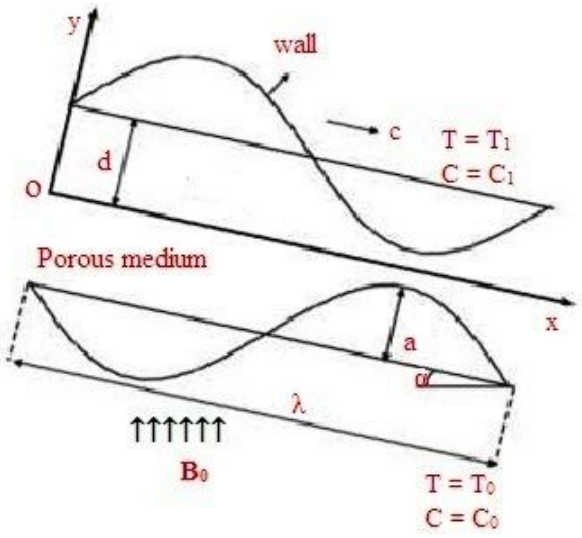

Figure 1: Schematic diagram of the physicalmodel

The equations governing the flow in wave frame of reference are given by

$$\frac{\partial u}{\partial x} + \frac{\partial v}{\partial y} = 0, \quad (2)$$

$$\rho\left[u\frac{\partial u}{\partial x} + v\frac{\partial u}{\partial y}\right] = -\frac{\partial p}{\partial x} + \mu\left[\frac{\partial^2 u}{\partial x^2} + \frac{\partial^2 u}{\partial y^2}\right] - \eta\left[\frac{\partial^4 u}{\partial x^4} + \frac{\partial^4 u}{\partial y^4} + 2\frac{\partial^4 u}{\partial x^2 \partial y^2}\right] - \left[\sigma {B_0}^2\right](u + c) - \left[\frac{\mu}{k_1}\right](u + c) + \rho g \sin\alpha, \quad (3)$$

$$\rho\left[u\frac{\partial v}{\partial x} + v\frac{\partial v}{\partial y}\right] = -\frac{\partial p}{\partial y} + \mu\left[\frac{\partial^2 v}{\partial x^2} + \frac{\partial^2 v}{\partial y^2}\right] - \eta\left[\frac{\partial^4 v}{\partial x^4} + \frac{\partial^4 v}{\partial y^4} + 2\frac{\partial^4 v}{\partial x^2 \partial y^2}\right] - \rho g \cos\alpha, \quad (4)$$

The energy equation is

$$\rho\, C_p\left[u\frac{\partial}{\partial x} + v\frac{\partial}{\partial y}\right]T = k\left[\frac{\partial^2}{\partial x^2} + \frac{\partial^2}{\partial y^2}\right]T + Q_0 + \sigma B_0^2 u^2 - \frac{\partial q_r}{\partial y}, \quad (5)$$

The concentration equation is

$$\left[u\frac{\partial C}{\partial x} + v\frac{\partial C}{\partial y}\right] = D_m\left[\frac{\partial^2 C}{\partial x^2} + \frac{\partial^2 C}{\partial y^2}\right] + \frac{D_m K_T}{T_m}\left[\frac{\partial^2 T}{\partial x^2} + \frac{\partial^2 T}{\partial y^2}\right] - k_2(C - C_0). \quad (6)$$

u and v are the velocity components in the corresponding coordinates, p is the fluid pressure, ρ is the density of the fluid, μ is the coefficient of the viscosity,$B_0$is the strength of the magnetic field, η is the coefficient of couple stress,$k_1$is the permeability of the porous medium, k is the thermal conductivity, Q_0 is the constant heat addition/absorption, C_p is the specific heat at constant pressure, σ is the electrical conductivity, g is the acceleration due to gravity ,α is inclination angle of the channel, T is the temperature, k_2 is the chemical reaction

of rate constant, C is the concentration of the fluid, D_m is the coefficient of mass diffusivity, T_m is the mean temperature and K_T is the thermal diffusion ratio.

Hence, for the Rossel and approximation for thermal radiation, we have

$$q_r = -\frac{16\,\sigma^* {T_0}^3}{3k^*}\frac{\partial T}{\partial y}, \tag{7}$$

where σ^* and k^* are the Stefan-Boltzmann constant and the mean absorption coefficient.

Introducing a wave frame (x, y) moving with velocity c away from the fixed frame (X, Y) by the transformation

$$x = X\text{-}ct,\ y = Y,\ u = U\text{-}c,\ v = V \text{ and } p(x) = P(X,t). \tag{8}$$

Introducing the following non-dimensional quantities:

$$\left.\begin{gathered}\overline{x} = \frac{x}{\lambda},\ \ \overline{y} = \frac{y}{d},\ \ \ \overline{t} = \frac{ct}{\lambda},\ \ \ \ \overline{u} = \frac{u}{c},\ \ \ \ \overline{v} = \frac{v}{c\delta},\ \ \overline{p} = \frac{d^2 p}{c\lambda\mu},\ \varepsilon = \frac{a}{d}, \delta = \frac{d}{\lambda},\\ Da = \frac{k_1}{d^2}, Re = \frac{\rho c d}{\mu},\ \ M = B_0 d\sqrt{\frac{\sigma}{\mu}},\ \ \ \Pr = \frac{\mu\, C_p}{\kappa},\ \beta = \frac{Q_0\, d^2}{\mu\, C_p (T_1 - T_0)},\\ \theta = \frac{\overline{T} - T_0}{T_1 - T_0}, \propto = \sqrt{\frac{\mu}{\eta}}d, \Phi = \frac{C - C_0}{C_1 - C_0},\ \ \eta_1 = \frac{\rho\, d^2 g}{\mu c},\ \ \eta_2 = \frac{\rho\, d^3 g}{\lambda\mu c},\ \ S_c = \frac{\mu}{D_m \rho},\\ S_r = \frac{D_m \rho\, k_T (T_1 - T_0)}{\mu T_m (C_1 - C_0)},\ R_n = \frac{16\,\sigma^* {T_0}^3 d^2}{3k^*\mu\, C_p},\ S = \frac{K_2 \rho\, a^2}{\mu},\end{gathered}\right\} \tag{9}$$

where $\epsilon = \frac{a}{d}$ is the non-dimensional amplitude of channel, $\delta = \frac{d}{\lambda}$ is the wave number, k_1 is the non - uniform parameter, Re is the Reynolds number, M is the Hartman number, $Da = \frac{k_1}{b^2}$ is the porosityparameter , $\propto$ is the couple stress parameter, η_1 and η_2 are gravitational parameters, Pr is the Prandtl number, ν is the heat source/sink parameter, Q_0 is the constant heat addition/absorption, R_n is the thermal radiation parameter, S_c Schmidt number, S_r is the Soret number and S is the Chemical reaction parameter.

3. Solution of the problem

In view of the above transformations (8) and non-dimensional variables (9), equations (2-6) are reduced to the following non-dimensional form after dropping the bars

$$\delta\left[\frac{\partial u}{\partial x} + \frac{\partial v}{\partial y}\right] = 0, \tag{10}$$

$$Re\delta\left[u\frac{\partial u}{\partial x} + v\frac{\partial u}{\partial y}\right] =$$

$$-\frac{\partial p}{\partial x} + \delta^2\frac{\partial^2 u}{\partial x^2} + \frac{\partial^2 u}{\partial y^2} - \frac{1}{\propto^2}\left(\delta^4\frac{\partial^4 u}{\partial x^4} + \frac{\partial^4 u}{\partial y^4} + 2\delta^2\frac{\partial^4 u}{\partial x^2 \partial y^2}\right) - Au - A + \eta_1 \sin\alpha, \tag{11}$$

$$Re\delta^3\left[u\frac{\partial v}{\partial x} + v\frac{\partial v}{\partial y}\right] =$$

$$-\frac{\partial p}{\partial y} + \delta^2\left(\delta^2\frac{\partial^2 v}{\partial x^2} + \frac{\partial^2 v}{\partial y^2}\right) - \frac{1}{\propto^2}\delta^2\left(\delta^4\frac{\partial^4 v}{\partial x^4} + \frac{\partial^4 v}{\partial y^4} + 2\delta^2\frac{\partial^4 v}{\partial x^2 \partial y^2}\right) - \eta_2\cos\alpha, \tag{12}$$

$$Re\left[\delta u\frac{\partial \theta}{\partial x} + v\frac{\partial \theta}{\partial y}\right] = \frac{1}{P_r}\left[\delta^2\frac{\partial^2 \theta}{\partial x^2} + \frac{\partial^2 \theta}{\partial y^2}\right] + \beta + M^2 E_c u^2 + R_n\frac{\partial^2 \theta}{\partial y^2}, \tag{13}$$

$$Re\delta\left[u\frac{\partial\phi}{\partial x}+v\frac{\partial\phi}{\partial y}\right]=\frac{1}{S_c}\left[\delta^2\frac{\partial^2\phi}{\partial x^2}+\frac{\partial^2\phi}{\partial y^2}\right]+S_r\left[\delta^2\frac{\partial^2\theta}{\partial x^2}+\frac{\partial^2\theta}{\partial y^2}\right]-k_2(C-C_0). \quad (14)$$

Applying long wave length approximation and neglecting the wave number along with low-Reynolds numbers. Equations (10 - 14) become

$$\frac{1}{\alpha^2}\frac{\partial^4 u}{\partial y^4}-\frac{\partial^2 u}{\partial y^2}+Au=-\frac{\partial p}{\partial x}-A+\eta_1\sin\alpha, \quad (15)$$

$$\frac{\partial p}{\partial y}=0, \quad (16)$$

$$\frac{1}{P_r}\frac{\partial^2\theta}{\partial y^2}+\beta+M^2E_cu^2+R_n\frac{\partial^2\theta}{\partial y^2}=0, \quad (17)$$

$$\frac{1}{S_c}\frac{\partial^2\phi}{\partial y^2}+S_r\frac{\partial^2\theta}{\partial y^2}-S\phi=0. \quad (18)$$

The dimensionless boundary conditions

$$\frac{\partial u}{\partial y}=0 \quad \frac{\partial^3 u}{\partial y^3}=0 \quad \text{at y = 0,} \quad (19)$$

$$\text{u = 0} \quad \frac{\partial^2 u}{\partial y^2}=0 \quad \text{at y = h(x, t) =1 + } \epsilon \sin\{2\pi(x-t)\}, \quad (20)$$

$$\theta = 0, \Phi = 0 \text{ at y = 0,} \quad (21)$$

$$\theta = 1, \Phi = 1 \text{ at y = h =1 + } \epsilon \sin\{2\pi(x-t)\}. \quad (22)$$

Solving equation (15) using the boundary conditions (19 and 20), we get

$$u=n_1cosh[\alpha_1 y]+n_2cosh[\alpha_2 y]-B, \quad (23)$$

where

$$n_1=\frac{B-n_2\cosh[\alpha_2 h]}{\cosh[\alpha_1 h]}, n_2=\frac{B{\alpha_1}^2}{({\alpha_1}^2-{\alpha_2}^2)\cosh[\alpha_2 h]}, B=\frac{1}{A}\left(\frac{dp}{dx}+A-\eta_1\sin\alpha\right),$$

$$\alpha_1=\sqrt{\frac{1+\sqrt{1-\left(\frac{4A}{\alpha^2}\right)}}{\left(\frac{2}{\alpha^2}\right)}}, \alpha_2=\sqrt{\frac{1-\sqrt{1-\left(\frac{4A}{\alpha^2}\right)}}{\left(\frac{2}{\alpha^2}\right)}}, A=\left(M^2+\frac{1}{Da}\right).$$

Solving Equations (17 and 18) with boundary conditions (21) and (22), we get

$$\theta = n_3+n_3y+(C-a_7)\frac{y^2}{2}-2a_1\cosh[2\alpha_1 y]-2a_2\cosh[2\alpha_2 y]$$

$$-2a_3\cosh[(\alpha_1+\alpha_2)y]-2a_4\cosh[(\alpha_1-\alpha_2)y]-2a_5\cosh[\alpha_1 y]$$

$$+2a_6\cosh[\alpha_2 y], \quad (24)$$

where

$$n_3=2\,a_1+2\,a_2+2\,a_3+2\,a_4+2\,a_5-2\,a_6,$$

$$n_4=1-n_3-\frac{Ch^2}{2}+2a_1\cosh[2\alpha_1 h]+2a_2\cosh[2\alpha_2 h]+2a_3\cosh[(\alpha_1+\alpha_2)h]$$

$$+2a_4\cosh[(\alpha_1-\alpha_2)h]+2a_5\cosh[\alpha_1 h]-2a_6\cosh[\alpha_2 h]+a_7\frac{h^2}{2},$$

$$a_1=\frac{Dn_1{}^2}{16\,\alpha_1{}^2}, a_2=\frac{Dn_2{}^2}{16\alpha_2{}^2}, a_3=\frac{D\,n_1n_2}{(\alpha_1+\alpha_2)^2}, \quad a_4=\frac{D\,n_1n_2}{(\alpha_1-\alpha_2)^2}, \quad a_5=\frac{B\,n_1}{\alpha_1{}^2}, \quad a_6=\frac{B\,n_2}{\alpha_2{}^2},$$

$a_7 = \left(\frac{{n_1}^2}{2} + \frac{{n_2}^2}{2} + B^2\right), C = \left(\frac{-p_r \beta}{1+R_n p_r}\right), D = \left(\frac{M^2 B_r}{1+R_n p_r}\right).$

$\Phi = n_5 \sinh[\beta y] + n_6 \cosh[\beta y] + a_{15} + a_{16} \cosh[2\alpha_1 y] + a_{17} \cosh[2\alpha_2 y] +$

$a_{18} \cosh[(\alpha_1 + \alpha_2)y] + a_{19} \cosh[(\alpha_1 - \alpha_2)y] + a_{20} \cosh[\alpha_1 y] - a_{21} \cosh[\alpha_2 y],$ (25)

where

$$n_5 = \left(\frac{1}{\sinh(ah)}\right)(1 - n_6 \cosh(ah) - a_{15} - a_{16} \cosh[2\alpha_1 h] - a_{17} \cosh[2\alpha_2 h])$$
$$+ \left(\frac{1}{\sinh(ah)}\right)(-a_{18} \cosh[(\alpha_1 + \alpha_2)h] - a_{19} \cosh[(\alpha_1 - \alpha_2)h] - a_{20} \cosh[\alpha_1 h])$$
$$+ \left(\frac{1}{\sinh(ah)}\right)(a_{21} \cosh[\alpha_2 h]),$$

$n_6 = -a_{15} - a_{16} - a_{17} - a_{18} - a_{19} - a_{20} + a_{21},$

$\beta = \sqrt{S\, S_c}, a_8 = S_c S_r (C - a_7), a_9 = 8{\alpha_1}^2 S_c S_r a_1, a_{10} = 8{\alpha_2}^2 S_c S_r a_2,$

$a_{11} = 2(\alpha_1 + \alpha_2)^2 S_c S_r a_3, a_{12} = 2(\alpha_1 - \alpha_2)^2 S_c S_r a_4, a_{13} = 2{\alpha_1}^2 S_c S_r a_5,$

$a_{14} = 2{\alpha_2}^2 S_c S_r a_6, a_{15} = \left(\frac{a_8}{S}\right), a_{16} = \frac{a_9}{4{\alpha_1}^2 - S}, a_{17} = \frac{a_{10}}{4{\alpha_2}^2 - S}, a_{18} = \frac{a_{11}}{(\alpha_1+\alpha_2)^2 - S}, a_{19} =$

$\frac{a_{12}}{(\alpha_1-\alpha_2)^2 - S}, a_{20} = \frac{a_{13}}{{\alpha_1}^2 - S}, a_{21} = \frac{a_{14}}{{\alpha_2}^2 - S}.$

The volumetric flow rate in the wave frame is defined by

$$q = \int_0^h u dy = \int_0^h (n_1 cosh[\alpha_1 y] + n_2 cosh[\alpha_2 y] - B) dy = B a_{22}, \quad (26)$$

where

$$a_{22} = \left(\frac{1 - \left(\frac{{\alpha_1}^2}{({\alpha_1}^2 - {\alpha_2}^2) \cosh[\alpha_2 h]}\right) \cosh[\alpha_2 h]}{\alpha_1 \cosh[\alpha_1 h]}\right) \sinh[\alpha_1 h]$$
$$+ \left(\frac{{\alpha_1}^2}{\alpha_2({\alpha_1}^2 - {\alpha_2}^2) \cosh[\alpha_2 h]}\right) \sinh[\alpha_2 h] - h.$$

The pressure gradient obtained from equation (26) can be expressed as

$$\frac{dp}{dx} = \left[\frac{qA}{a_{22}} - A + \eta_1 \sin\alpha\right]. \quad (27)$$

The instantaneous flux Q (x, t) in the laboratory frame is

$$Q(x, t) = \int_0^h (u + 1) dy = q + h. \quad (28)$$

The average volume flow rate over one wave period (T = λ/c) of the peristaltic wave is defined as

$$\bar{Q} = \frac{1}{T} \int_0^T Q dt = q + 1. \quad (29)$$

From the equations (27) and (29), the pressure gradient can be expressed as

$$\frac{dp}{dx} = \left[\frac{(\bar{Q}-1)A}{a_{22}} - A + \eta_1 \sin\alpha\right]. \quad (30)$$

The dimensionless pressure rise per one wavelength in the wave frame is defined as

$$\Delta p = \int_0^1 \frac{dp}{dx}\, dx \tag{31}$$

The dimensionless friction force F at the wall across one wavelength is given by

$$F = \int_0^1 h\left(-\frac{dp}{dx}\right) dx. \tag{32}$$

4. Discussion of the problem

The main object of this investigation has been to study the joule heating and thermal radiation effects on MHD peristaltic couple stress hemodynamic fluid model through an inclined channel with chemical reaction. The numerical and computational results are discussed through the graphical illustration. **Mathematica** software is used to find out numerical results.

Pumping characteristics

4.1. Pressure rise

The pressure rise against the volume flow rate for different parameters of interest is demonstrated in figures (2) to (4). In these figures the region is divided into four parts: Retrograde pumping region ($\Delta p > 0, \overline{Q} < 0$), peristaltic pumping region ($\Delta p > 0, \overline{Q} > 0$), free pumping region ($\Delta p = 0$) and augmented region ($\Delta p < 0, \overline{Q} > 0$).The following default parameter values are adopted for computations: t = 0.2, ε = 0.2, $\alpha = \pi/3$, M = 0.5, Da = 0.05, η_1 = 0.5.Figure (2) portrayed that the pressure rise versus volumetric flow rate$\overline{Q}$. We notice from this graph that the pumping rate $\overline{Q}$ reduces in the entire retrograde ($\Delta p > 0, \overline{Q} < 0$) region and also in peristaltic pumping ($\Delta p > 0, \overline{Q} > 0$) zone while the pumping rate gradually increases in free pumping ($\Delta p = 0$) and co-pumping ($\Delta p < 0, \overline{Q} > 0$) zones by increase in porosity parameter Da (Da = 0.05, 0.1, 0.15) with fixed other parameters.The effect of Hartmann number (M) on pressure rise (Δp) is shown in figure (3).We notice that the pumping rate enhances in retrograde ($\Delta p > 0, \overline{Q} < 0$) region while the pumping rate reduces in peristaltic pumping ($\Delta p > 0, \overline{Q} > 0$), free pumping ($\Delta p = 0$) and co-pumping ($\Delta p < 0, \overline{Q} > 0$) zones by increase in Hartmann number (M = 0.5. 1.5, 2.5).Impact of couple stress parameter ($\propto$) on pressure rise (Δp) is plotted in figure (4). It is interesting to note that an increase in couple stress parameter ($\propto$ = 10, 20, 30),the pumping rate reduces in the entire retrograde ($\Delta p > 0, \overline{Q} < 0$) , peristaltic pumping ($\Delta p > 0, \overline{Q} > 0$) and free pumping ($\Delta p = 0$) zones while the pumping rate gradually increases in co-pumping ($\Delta p < 0, \overline{Q} > 0$)zone.

4. 2. Friction force

Figures (5) to (7) describe the variation of frictional force F against the flow rate for different parameters of interest like porosity parameter (Da), Hartmann Number (M) and couple stress parameter ($\propto$). The frictional forces exactly have an opposite behavior when compared to the pressure rise.

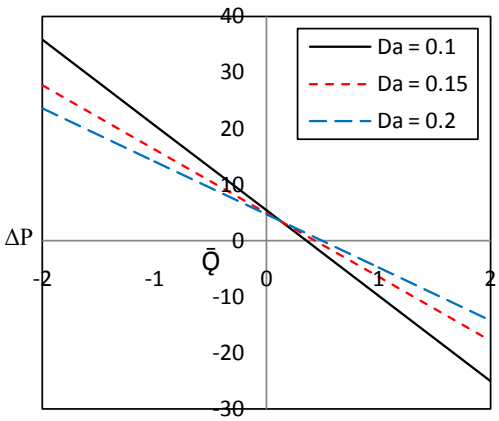

Figure 2: Impact of Da on Pressure rise

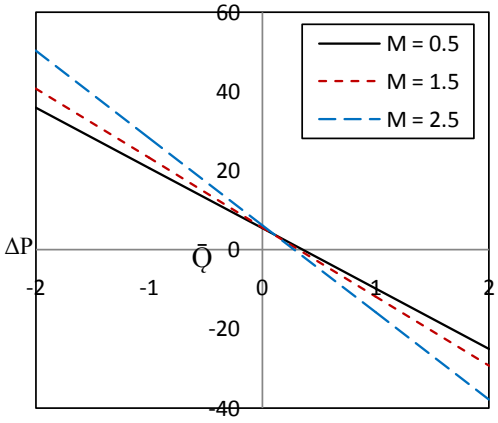

Figure 3: Impact of M on Pressure rise

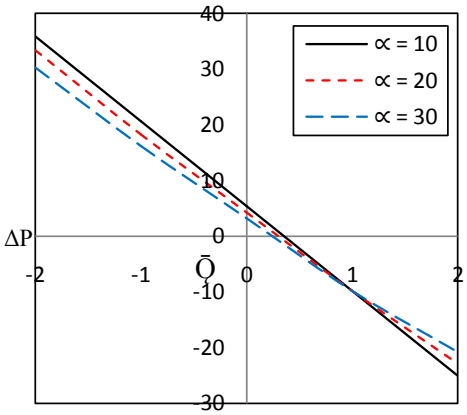

Figure 4: Impact of ∝ on Pressure rise

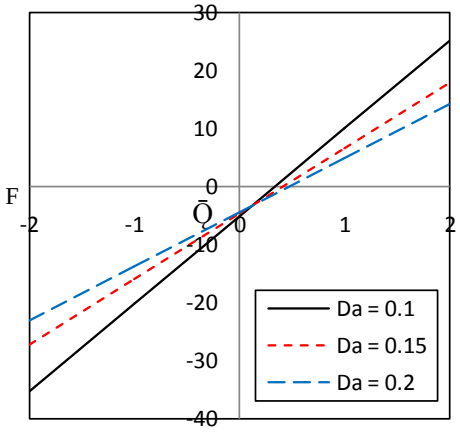

Figure 5: Impact of Da on Friction force

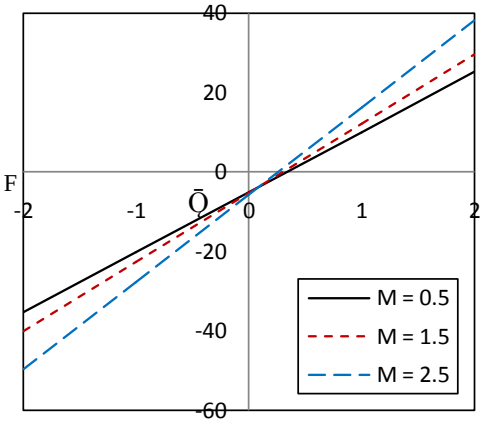

Figure 6: Impact of M on Friction force

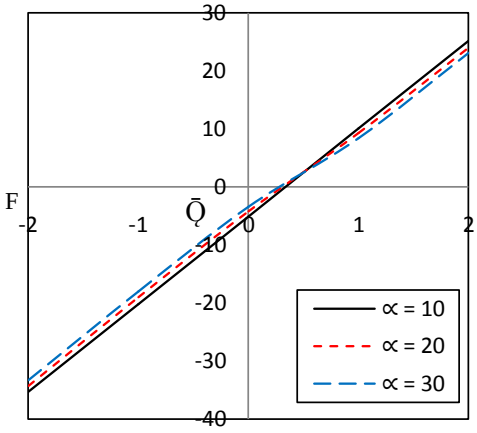

Figure 7: Impact of ∝ on Friction force

4.3. Heat transfer Analysis

Variations of temperature distribution (θ) with respect to y for various values of interest like porosity parameter (Da), prandtl number (Pr), heat source parameter (β),thermal radiation parameter (Rn), hartmann number (M), brinkman number and couple stress parameter (∝)are shown in figures 8 -14. The following default parameter values are adopted for computations: ε = 0.2, t = x = 0.2, p = 0.1, $\alpha = \pi/3$,η_1 = 0.5, M = 0.5, Da = 0.05, ∝ = 10, Pr = 3, Br = 1, Rn = 0.3, β = 0.5. Figure (8) reveals that the effect of porosity parameter on temperature distribution (θ). We perceive from this graph that an increase in porosity parameter (Da = 0.05, 0.1, 0.15), the results in temperature profile reduces.Effect of prandtl number (Pr) on the temperature of the fluid (θ) is presented in figure (9). It is clear that the temperature of the fluid enhances with an increase in prandtl number (Pr = 3, 6, 9) with fixed other parameters. Figure (10) presents the various values of heat source/sink parameter (β) on temperature profile (θ). We notice that the temperature of the fluid increases significantly by the increase in heat source/sink parameter (β = 0.1, 0.3, 0.5).Fig. 11 elucidates the influence of thermal radiation parameter on temperature distribution. Indeed, the temperature of the fluid reduces by increase in thermal radiation parameter (Rn = 0.3, 0.6, 0.9).The relation between temperature and hartmann number is presented in figure (12).We observe from this graph that the temperature of the fluid gradually rises by an increase in hartmann number (M = 0.5, 1.5, 2.5) with fixed other parameters. This enhancement in temperature due to consideration of Joule heating and also we notice that enhancement in the temperature profile is not noteworthy.Figure 13 is sketched for various values of brinkman number (Br) over the temperature of the fluid. This figure indicates that the results in the temperature of the fluid increase with an increase inbrinkman number (Br = 1, 1.5, 2.5).Figure 14 describes the behaviour of couple stress parameter effect on temperature distribution. It is seen clearly from the figure that, as couple stress parameter increases, results in temperature profile enhances.

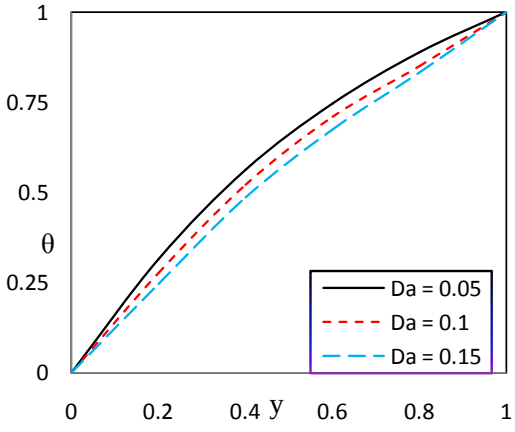

Figure 8: Impact of Da on Temperature

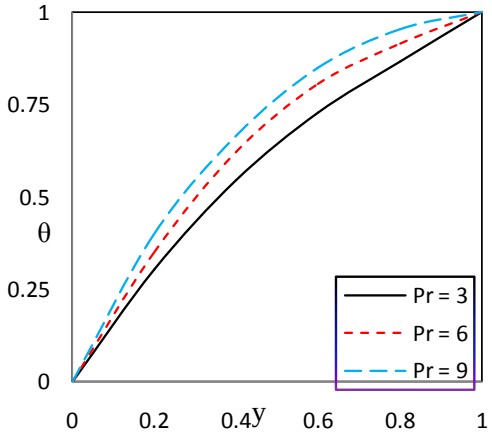

Figure 9: Impact of Pr on Temperature

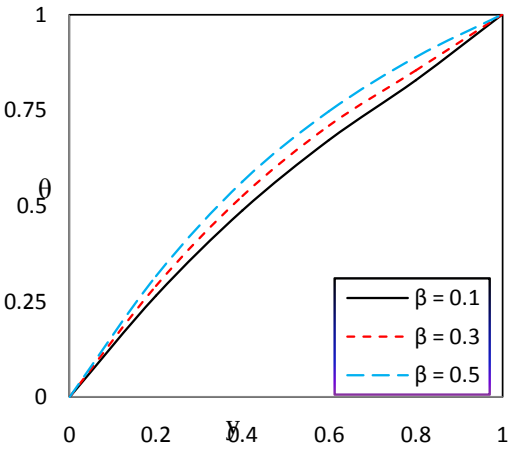

Figure 10: Impact of β on Temperature

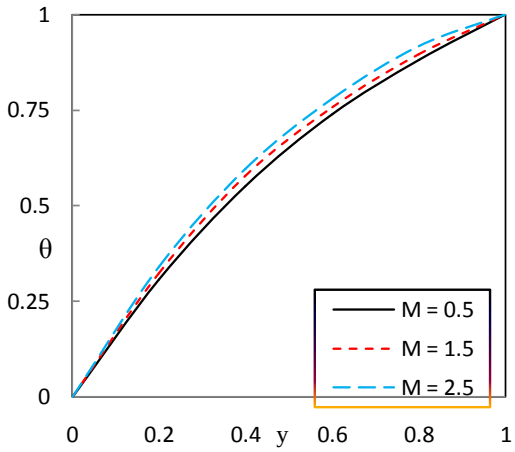

Figure 12: Impact of M on Temperature

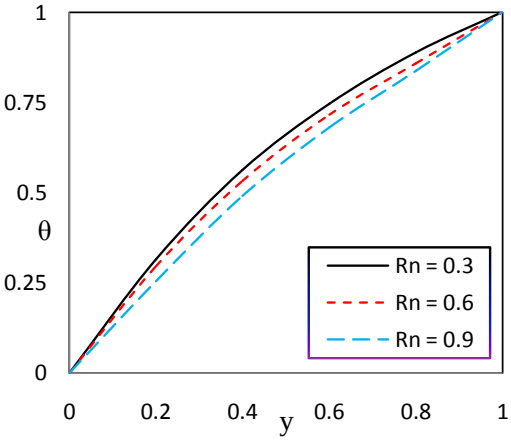

Figure 11: Impact of Rn on Temperature

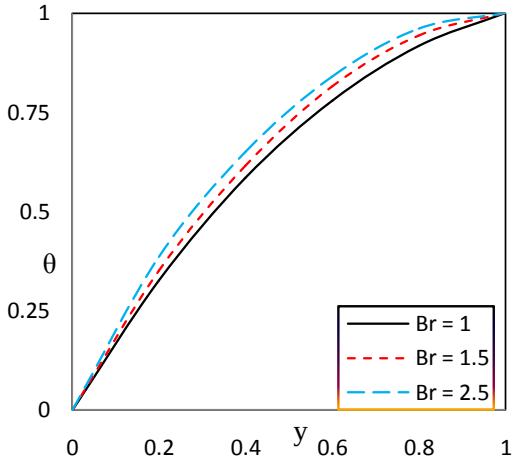

Figure 13: Impact of Br on Temperature

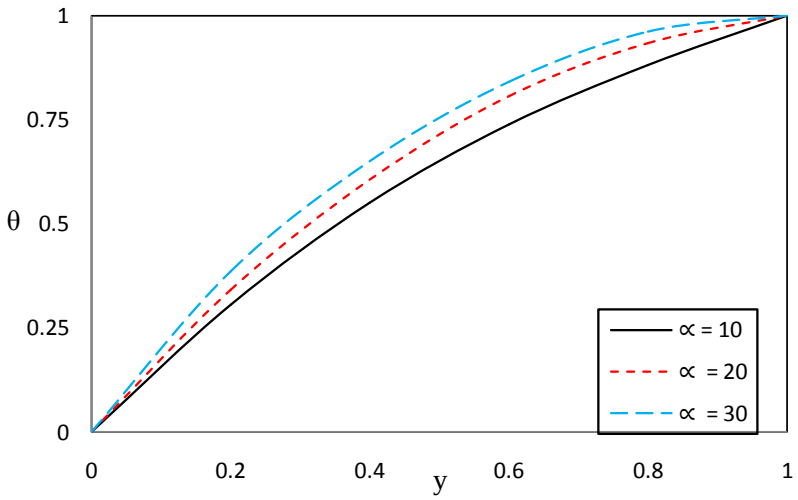

Figure 14: Impact of $\propto$ on Temperature

4.4. Mass transfer analysis

The influence of Schmidt number (Sc), Soret number (Sr), Prandtl number (Pr), Thermal radiation parameter (Rn), Hartmann number (M), Porosity parameter (Da), Chemical reaction parameter (S) and Couple stress parameter (∝)on concentration distribution are shown graphically in figures 15-22. The following default parameter values are adopted for computations: ε = 0.2, t = x = 0.2, p = 0.1, $\alpha = \pi/3, \eta_1 = 0.5$, M = 0.5, Da = 0.1, ∝ = 10,Pr = 3, Br = 1, Rn = 0.3, β = 0.5,S = 2,Sc = 1.5,Sr = 3.5.Effect of Schmidt number (Sc) on concentration profile is depicted in figure (15). It is clear from this graph that the results in concentration profile decrease by an increase in Schmidt number (Sc = 0.5, 1, 1.5) with fixed other parameters.The relation between concentration distribution (Φ) and porosity parameter has been presented in figure (16). It can be seen that an increase in Soret number (Sr = 1.5, 3.5, 5.5) causes reduces concentration distribution.Figure (17) displays the variation of Prandtl number (Pr) on concentration distribution. We notice from this graph that an increase in Prandtl number (Pr = 3, 6, 9) causes reduction of concentration distribution because a rise Pr enriches viscosity of the fluid which turns degeneration the concentration of the fluid.Impact of thermal radiation parameter (Rn) on concentration distribution (Φ) is depicted in figure (18). We observe that the concentration profile of the fluid enhances by an increase in thermal radiation parameter (Rn = 0.3, 0.6, 0.9) with fixed other parameters.Figures (19 and 20) illustrate the effect of Hartmann number (M) and Couple stress parameter (∝) on concentration distribution. We observe from these graphs that the concentration distribution of the fluid reduces by an increase in Hartmann number (M = 0.5, 1.5, 2.5) and Couple stress parameter (∝ = 10, 20, 30).Impact of porosity parameter (Da) and chemical reaction parameter (S) on concentration distribution are presented in figures (21&22). It is clear from these graphs that the results in concentration profile enhances by increase in porosity parameter (Da = 0.05, 0.1, 0.15) and chemical reaction parameter (S = 0.5, 2, 2.5) and also we notice that the fluid flow in concentration distribution is not significant by increase in porosity parameter (see figure 21).

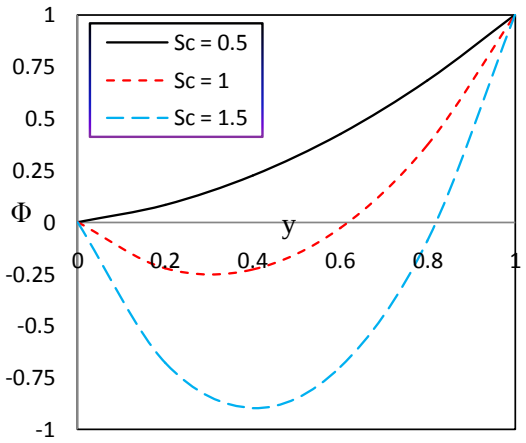

Figure 15: Impact of Sc on Concentration profile

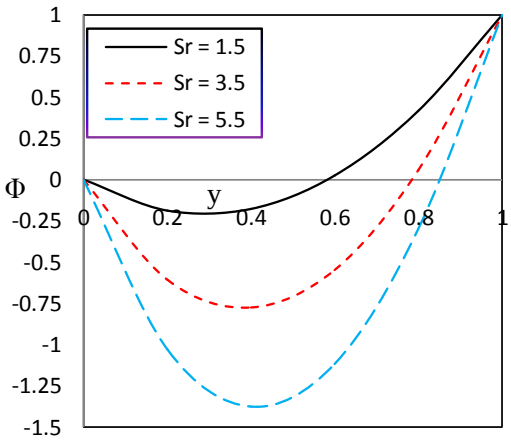

Figure 16: Impact of Sr on Concentration profile

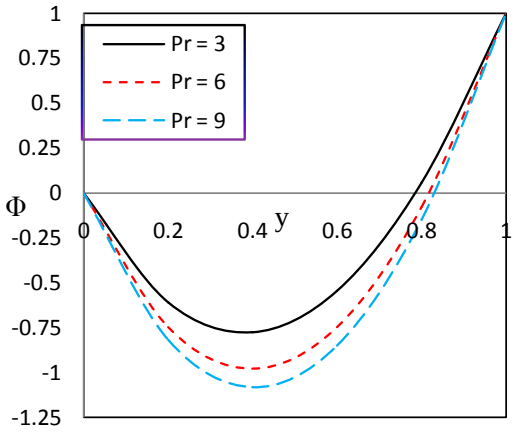

Figure 17: Impact of Pr on Concentration profile

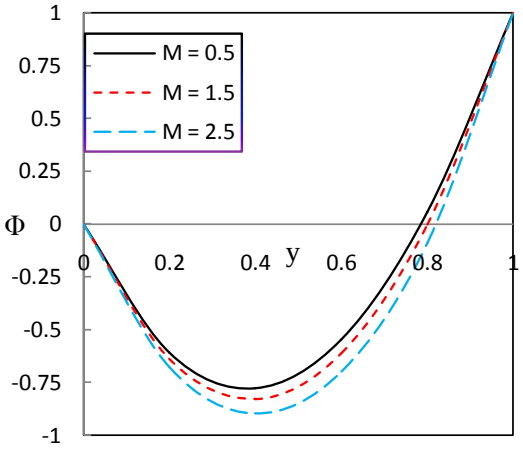

Figure 19: Impact of M on Concentration profile

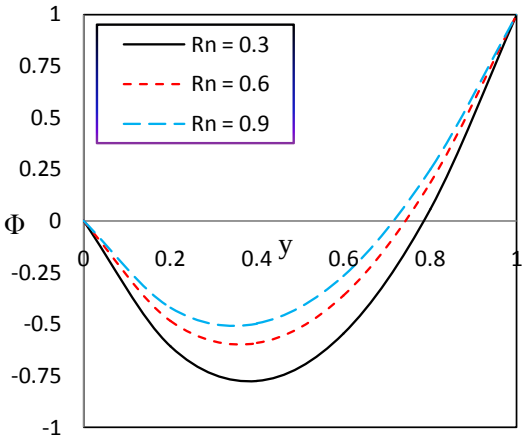

Figure 18: Impact of Rn on Concentration profile

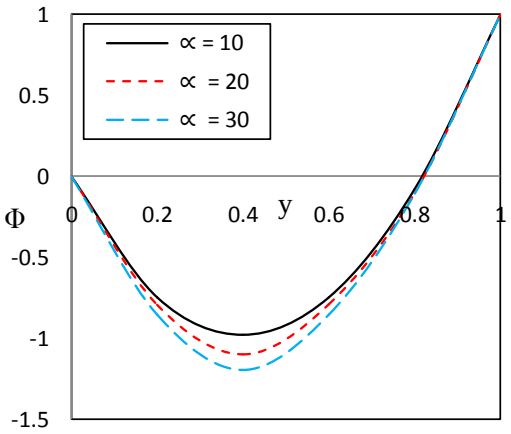

Figure 20: Impact of ∝ on Concentration profile

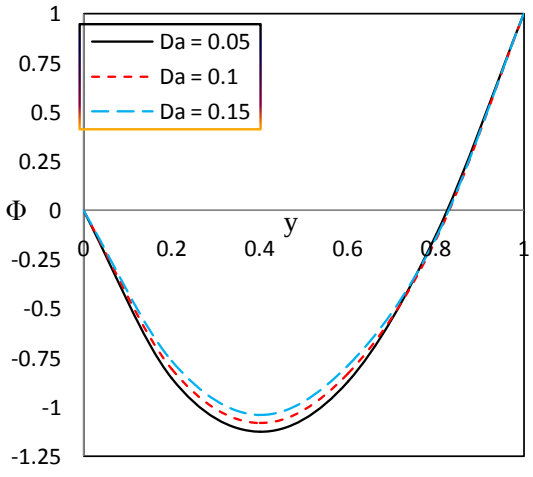

Figure 21: Impact of Da on Concentration profile

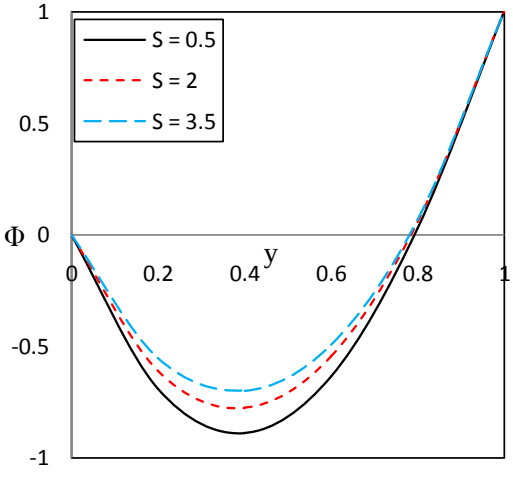

Figure 22: Impact of S on Concentration profile

5. Conclusions

Joule heating and thermal radiation effects on MHD peristaltic couple stress hemodynamic fluid model through an inclined channel with chemical reaction have been investigated. The porous medium is also taken into the account. The main findings are cited below.

1. Pumping rate $\overline{Q}$ reduces in the entire retrograde ($\Delta p > 0, \overline{Q} < 0$) region and also in peristaltic pumping ($\Delta p > 0, \overline{Q} > 0$) zone while the pumping rate gradually increases in free pumping ($\Delta p = 0$) and co-pumping ($\Delta p < 0, \overline{Q} > 0$) zones by increase in porosity parameter (Da).
2. Pumping rate reduces in the entire retrograde ($\Delta p > 0, \overline{Q} < 0$) , peristaltic pumping ($\Delta p > 0, \overline{Q} > 0$) and free pumping ($\Delta p = 0$) zones while the pumping rate gradually increases in co-pumping ($\Delta p < 0, \overline{Q} > 0$)zone by increase in Hartmann number (M).
3. Frictional forces exactly have an opposite behavior when compared to the pressure rise.
4. Temperature of the fluid enhances by increase in Hartmann number (M), Prandtl number (Pr), Brinkman number (Br), heat source/sink parameter (β) and couple stress parameter ($\propto$) while it reduces by increase in porosity parameter (Da) and thermal radiation parameter (Rn).
5. Concentration of the fluid increases by increase in thermal radiation parameter (Rn), porosity parameter (Da) and chemical reaction parameter (S) while it decreases by increase in schmidt number (Sc), Soret number (Sr), prandtl number (Pr),Hartmann number (M)and couple stress parameter($\propto$).

References

[1] F.Kill,The function of the urethra and the Renal Pelvis, Saunders, Philadelphia, (1957).

[2] T.W.Lathem,Fluid motion in a peristaltic pump. M S. Thesis. Massachusetts Institute of Technology, Cambridge, M.A. (1966)

[3] A.H.Shapiro, M.Y. Jaffrin, M.Y. and S.L.Weinberg,Peristaltic pumping with long wavelengths at low Reynolds number,*J. Fluid Mech.*,**37**(1969), 799-825.

[4] D. Shrinivasacharya, M. Mishra and A.R. Rao,Peristaltic pumping of a Micropolar fluid in a tube,*Acta Mech*, **161** (2003), 165–178.

[5] K. Vajravelu, G. Radhakrishnamacharya and V. Radhakrishnmurthy, Peristaltic flow and heat transfer in a vertical porous annulus with long wave approximation,*Int. J. Non-Linear Mech*, **42** (2007), 754–759.

[6] S. Maiti, S. and J.C. Misra,Peristaltic transport of a couple stress fluid: Some applications to hemodynamics,*J. Mech. Med. Biol.*, **12** (2012),1250048.

[7] S. Ravikumar,Effect of couple stress fluid flow on magnetohydrodynamic peristaltic blood flow with porous medium trough inclined channel in the presence of slip effect-Blood flow study,*International Journal of Bio-Science and Bio-Technology*, **7**, No.5 (2015), 65-84.

[8] S. Ravikumar, Analysis of heat transfer on MHD peristaltic blood flow with porous medium through coaxial vertical tapered asymmetric channel with radiation -blood flow study,International Journal of Bio-Science and Bio-Technology, **8**, No.2 (2016), 395-408.

[9] S. Ravikumar,Hydromagnetic peristaltic transportation with porous medium through coaxial asymmetric vertical tapered channel and joule heating,*AAM: Intern. J.*, **11,** No.2 (2016), 735-747.
[10] S. Ravikumar and S.K. Abzal,Combined influence of hall currents and joule heating on hemodynamicperistaltic flow with porous medium through a vertical tapered asymmetric channel with radiation,*Frontiers in Heat and Mass Transfer (FHMT)*,**9** – **19**(2017), 1 – 9.
[11] N. Ameer Ahamad,S. Ravikumar and Kalimuthu Govindaraju, Influence of radiation on MHD peristaltic blood flow through a tapered channel in presence of slip and joule heating,*AIP Conference Proceedings*,**1863**(2017), 560091-1 - 560091-5.
[12] G.C.Sankadand P.S. Nagathan,Transport of MHD couple stress fluid through peristalsis in a porous medium under the influence of heat transfer and slip effects,*Int. J. of Applied Mechanics and Engineering*,**22**, No. 2(2017), 403-414.
[13] G.C. Shit andM. Roy, Hydromagnetic effect on inclined peristaltic flow of a couple stress fluid,*Alexandria Engineering Journal*, **53**, No.4 (2014), 949–958.
[14] K.H.Kabir, M. A. Alim and L. S. Andallah, Effects of stress work on MHD natural convection flow along a vertical wavy surface with Joule heating,*Journal of Applied Fluid Mechanics*,**8**, (2015), 213-221.
[15] T.Hayat, S. Farooq, B. Ahmad and A. Alsaedi,Characteristics of convective heat transfer in the MHD peristalsis of Carreau fluid with Joule heating,*AIP Advances*, **6** (2016), 045302
[16] F.M. Abbasi, T. Hayat and A. Alsaedi,Effects of inclined magnetic field and Joule heating in mixed convective peristaltic transport of non-Newtonian fluids,*Bulletin of the polish academy of sciences technical sciences*, **63**, No.2 (2015), 501-514.
[17] M. Kothandapani andJ. Prakash, Influence of thermal radiation and magnetic field on peristaltic transport of a Newtonian nanofluid in a tapered asymmetric porous channel,*Journal of nanofluids*, **5**, No. 3 (2016), 363-374.
[18] K. Ramesh,Influence of heat and mass transfer on peristaltic flow of a couple stress fluid through porous medium in the presence of inclined magnetic field in an inclined asymmetric channel,*J Mol Liq*, **219**, (2016), 256 -71.
[19] T. Hayat, A. Saima Rani, Alsaediand M. Rafiq, Radiative peristaltic flow of magneto nanofluid in a porous channel with thermal radiation,*Results in Physics*, **7** (2017), 3396 -3407.
[20] K. Maruthi Prasad, N. Subadra and M.A.S. Srinivas, Heat and mass transfer effects of peristaltic transport of a nanofluid in peripheral layer, *AAM: Intern. J.*, **12**, No.2 (2017), 968-987.
[21] A.Mohan Rami Reddy, J.V. Ramana Reddy N. Sandeep and V. Sugunamma,Effect of nonlinear thermal radiation on MHD chemically reacting maxwell fluid flow past a linearly stretching sheet studied,*AAM: Intern. J.*, **12**, No.1 (2017), 259-274.
[22] E.P.Siva and A.Govindarajan, Soret effect on peristaltic flow of a couple stress fluid in a tapered channel, *International Journal of Pure and Applied Mathematics*,**113,** No. 9 (2017), 66 – 74.
[23] R Latha , B. Rushi Kumar, MHD peristaltic flow of a couple stress fluid in an asymmetric channel, *International Journal of Pure and Applied Mathematics*,**113,** No. 8 (2017), 37 – 45.